Published in final edited form as:
Nat Med. ; 17(12): 1668–1673. doi:10.1038/nm.2490.

Stimulating healthy tissue regeneration by targeting the 5-HT_{2B} receptor in chronic liver disease

Mohammad R Ebrahimkhani[1,2,6], **Fiona Oakley**[1,6], **Lindsay B Murphy**[1], **Jelena Mann**[1], **Anna Moles**[1], **Maria J Perugorria**[1], **Elizabeth Ellis**[1], **Anne F Lakey**[1], **Alastair D Burt**[1], **Angela Douglass**[1], **Matthew C Wright**[1], **Steven A White**[1], **Fabrice Jaffré**[3,4,5], **Luc Maroteaux**[3,4,5], and **Derek A Mann**[1]

[1]Fibrosis Laboratory, Liver Group, Institute of Cellular Medicine, Newcastle University, Newcastle Upon Tyne, UK

[2]Massachusetts Institute of Technology Center for Environmental Health Sciences, Department of Biological Engineering, Department of Biology, Massachusetts Institute of Technology, Cambridge, Massachusetts, USA

[3]Institut National de la Santé et de la Recherche Médicale Unité Mixte de Recherche S 839, Paris, France

[4]Université Pierre et Marie Curie, Paris, France

[5]Institut du Fer à Moulin, Paris, France

Abstract

Tissue homeostasis requires an effective, limited wound-healing response to injury. In chronic disease, failure to regenerate parenchymal tissue leads to the replacement of lost cellular mass with a fibrotic matrix. The mechanisms that dictate the balance of cell regeneration and fibrogenesis are not well understood[1]. Here we report that fibrogenic hepatic stellate cells (HSCs) in the liver are negative regulators of hepatocyte regeneration. This negative regulatory function requires stimulation of the 5-hydroxytryptamine 2B receptor (5-HT_{2B}) on HSCs by serotonin, which activates expression of transforming growth factor β1 (TGF-β1), a powerful suppressor of hepatocyte proliferation, through signaling by mitogen-activated protein kinase 1 (ERK) and the transcription factor JunD. Selective antagonism of 5-HT_{2B} enhanced hepatocyte growth in models of acute and chronic liver injury. We also observed similar effects in mice lacking 5-HT_{2B} or JunD or upon selective depletion of HSCs in wild-type mice. Antagonism of 5-HT_{2B} attenuated fibrogenesis and improved liver function in disease models in which fibrosis was pre-established and progressive. Pharmacological targeting of 5-HT_{2B} is clinically safe in humans and may be therapeutic in chronic liver disease.

Correspondence should be addressed to D.A.M. (derek.mann@ncl.ac.uk)..
[6]These authors contributed equally to this work

AUTHOR CONTRIBUTIONS

M.R.E. and F.O. performed the majority of the experiments with assistance from L.B.M., J.M., E.E., A.D., M.C.W., F.J., A.M., M.J.P., A.F.L. and L.M. A.D.B. determined the fibrosis scores in the mouse models of liver injury. S.A.W. supplied the human liver tissue for the isolation of hepatocytes and stellate cells. D.A.M. and F.O. conceived of the study, planned the experiments and wrote the paper.

Note: Supplementary information is available on the Nature Medicine website.

COMPETING FINANCIAL INTERESTS

The authors declare competing financial interests: details accompany the full-text HTML version of the paper at http://www.nature.com/naturemedicine/.

Europe PMC Funders Author Manuscripts

Diminished hepatocyte regeneration is a feature of liver disease and is associated with fibrogenesis that leads to the development of liver cirrhosis and cancer[2-4]. Regulation of hepatocyte proliferation is complex and involves crosstalk between resident non-parenchymal and parenchymal cells, with an additional influence from recruited hematopoietic cells[5]. As a result of this complexity, it is incompletely understood how hepatocyte proliferation is regulated. For example, the contribution of HSCs has not been established[6]. In the diseased liver, HSCs transdifferentiate into 'activated' myofibroblasts that then drive fibrogenesis by promoting the net deposition of extracellular matrix[2,6]. HSCs also secrete numerous soluble factors that might influence hepatocyte proliferation, including hepatocyte growth factor (HGF), TGF-β1 and interleukin-6 (IL-6)[2,6]. Previous studies suggested stimulatory functions for HSCs in hepatocyte regeneration, however, no conclusive *in vivo* evidence has been provided[7,8]. As activated HSCs are continually generated in diseased liver, it is crucial to define their influence on tissue regeneration.

Bile duct obstruction occurs in a variety of clinical settings and can cause cholestatic injury, including hepatocyte death and fibrosis[9]. Bile duct ligation (BDL) is an established model of extrahepatic cholestasis in rodents[10]. We determined the effects of selective apoptosis-mediated depletion of HSCs on hepatocyte proliferation in mice with pre-established and ongoing progressive BDL-induced liver damage, a condition in which fibrogenesis and parenchymal tissue regeneration are concurrent ongoing processes that influence disease progression. We targeted HSCs with administration of the single-chain antibody C1-3 conjugated to gliotoxin, which is a potent pro-apoptotic fungal metabolite[11-13]. C1-3 recognizes the antigen synaptophysin, which is expressed on myofibroblasts positive for α-smooth muscle actin (α-SMA$^+$ myofibroblasts) derived from transdifferentiation of HSCs. Notably, a previous study did not detect synaptophysin in any other liver cell type or in α-SMA$^+$ myofibroblasts derived from any other cell type in diseased rat liver[14]. The *in vivo* administration of C1-3–gliotoxin in the BDL model should therefore selectively deplete HSC-derived myofibroblasts and should not affect the number of myofibroblasts generated from portal-tract fibroblasts. Accordingly, we observed a substantive but incomplete depletion of hepatic α-SMA$^+$ cells in mice treated with C1-3–gliotoxin (Fig. 1a). A control single-chain antibody conjugate (CSBD9-gliotoxin) had no influence on hepatocyte proliferation, and staining for the transmembrane protein F4/80 and cytokeratin 19 (CK19) confirmed that C1-3–gliotoxin did not significantly modulate the number of Kupffer cells or cholangiocytes (Fig. 1b and Supplementary Fig. 1a). Proliferating cell nuclear antigen (PCNA) staining of liver sections revealed that treatment with C1-3–gliotoxin stimulated hepatocyte proliferation (Fig. 1c). Depletion of HSCs was not associated with changes in the expression of the hedgehog target gene *Gli2* (Supplementary Fig. 1a), ruling out activation of the hedgehog pathway as a mechanism by which apoptotic depletion of HSCs stimulates hepatocyte growth[15].

We then investigated paracrine signaling between HSCs and hepatocytes, which might explain the antiregenerative properties of HSCs. Platelet-derived serotonin (5-HT) regulates liver regeneration through the 5-HT$_2$ subclass (comprising 5-HT$_{2A}$, 5-HT$_{2B}$ and 5-HT$_{2C}$) of serotonin receptors[16]. However, recently, 5-HT has been shown to be produced by cholangiocytes and to limit biliary cell proliferation in an autocrine manner[17]. This observation suggests that the serotonin signaling system can exert both proliferative and antiproliferative effects on parenchymal cells. We recently identified functional 5-HT$_{2B}$ receptors on activated HSCs in diseased liver[18]. Therefore, it was of interest to determine whether 5-HT$_{2B}$ influences hepatocyte regeneration in the context of liver injury, where the presence of 5-HT$_{2B}$ on HSCs might be particularly relevant. To address this issue, we used the drug SB-204741, a highly specific molecular antagonist of 5-HT$_{2B}$ that has negligible effects on 5-HT$_{2A}$ or 5-HT$_{2C}$ (ref. 19). Administration of SB-204741 stimulated hepatocyte proliferation in progressive BDL-induced liver injury and in liver damage induced by acute

carbon tetrachloride (CCl_4) (Fig. 1d,e). We observed no significant effects of SB-204741 on expression of the hepatomitogen hepatocyte growth factor (HGF) (Supplementary Fig. 1b), cholangiocyte proliferation or hedgehog signaling (Supplementary Fig. 1c). Furthermore, the selective 5-HT_{2A} and 5-HT_{2C} antagonist ketanserin had no effect on hepatocyte proliferation in CCl_4-injured liver, indicating a specific regulatory role for 5-HT_{2B} in this model (Fig. 1e)[20].

To confirm the antiregenerative influence of 5-HT_{2B} signaling, we compared hepatocyte proliferation in *Htr2b*$^{-/-}$ (5-HT_{2B} knockout) and wild-type mice after partial hepatectomy (PHX). Uninjured 5-HT_{2B} knockout mice showed no structural or biochemical evidence of liver defects (Supplementary Fig. 2a). Hepatocyte proliferation, measured by three independent protocols, was elevated in 5-HT_{2B}–deficient mice at 36 h and 72 h after PHX (Fig. 2a–c). IL-6 and TNF-α are primers of hepatocyte regeneration that are expressed transiently within hours after surgery[5,21]; expression of both of these factors was modestly increased in 5-HT_{2B} knockout mice at 4 h after surgery (Fig. 2d,e). TGF-β1 is induced in the termination phase of liver regeneration and functions as a repressor of hepatocyte proliferation[5,21], and we found that TGF-β1 expression was induced at 36 h after surgery and remained elevated at 72 h after surgery in livers from wild-type mice. However, TGF-β1 was not induced in the livers of 5-HT_{2B} knockout mice, but, instead, expression was diminished at these time points when compared with sham-injured mice (Fig. 2f). To corroborate these data, we repeated PHX in wild-type mice treated with SB-204741 or ketanserin[20]. We observed increased liver-to-body-weight ratios at up to 7 d after surgery in mice treated with SB-204741 compared to the mice treated with vehicle or ketanserin (Fig. 2g). This result indicates that selective antagonism of 5-HT_{2B} leads to a sustained stimulation of liver regeneration. Staining for Ki67 and for PCNA showed an increased number of proliferating hepatocytes in livers treated with SB-204741 (Fig. 2h and Supplementary Fig. 2b). In contrast, treatment with ketanserin reduced the number of Ki67$^+$ cells, confirming the results from a previous report showing that serotonin stimulates liver regeneration through 5-HT_{2A} (ref. 16). Treatment with SB-204741 also repressed hepatic TGF-β1 expression compared with the control and ketanserin groups in which TGF-β1 mRNA expression was elevated at 36 and 72 h (Fig. 2i).

5-HT_{2B} is expressed in diseased liver on HSCs, and at lower levels on cholangiocytes and Kupffer cells (Supplementary Fig. 2c,d). We also found 5-HT_{2B} to be induced in HSCs after PHX (Fig. 3a), whereas the expression of 5-HT_{2B} in hepatocytes was reduced (Supplementary Fig. 2e). Treatment with C1-3–gliotoxin enhanced hepatocyte proliferation after PHX, and this enhancement was accompanied by the diminished hepatic expression of TGF-β1 (Fig. 3b). As in the BDL model, depletion of HSCs did not alter the number of F4/80$^+$ Kupffer cells or CK19$^+$ cholangiocytes and had no effect on progenitor cell proliferation or hedgehog signaling (Supplementary Fig. 3). Given the similarity between the effects of HSC depletion and antagonism of 5-HT_{2B} on hepatocyte proliferation in multiple injury models, it seemed likely that HSCs control the antiregenerative effects of 5-HT_{2B}. If, however, HSC depletion and 5-HT_{2B} antagonism stimulate hepatocyte proliferation through independent mechanisms, then the combined depletion of HSCs and treatment with SB-204741 would be expected to result in additive stimulatory effects (Fig. 3c). We tested this hypothesis in mice at 48 h after CCl_4 injury, because we found HSCs to be maximally activated at this time point (Supplementary Fig. 4a). We again observed that HSC depletion and 5-HT_{2B} antagonism each enhanced hepatocyte proliferation and inhibited TGF-β1 expression (Fig. 3d), and we saw no significant changes in the expression of α fetoprotein (AFP), CK19, Gli2 or F4/80 (Supplementary Fig. 4b) or in the extent of liver injury (Supplementary Fig. 4c). Of note, there were no additive effects after combining HSC depletion with 5-HT_{2B} antagonism.

Hepatic TGF-β1 is predominantly expressed by HSCs and Kupffer cells. Serotonin treatment of cultured primary mouse HSCs increased the expression of TGF-β1, and this increase was inhibited by treatment with SB-204741 (Fig. 3e). In contrast, TGF-β1 expression in cultured mouse Kupffer cells was repressed by treatment with 5-HT, and treatment with SB-204741 prevented this repression but had no direct stimulatory effect (Fig. 3f). Therefore, given the specificity of C1-3 to HSC-derived α-SMA$^+$ myofibroblasts, our data strongly indicate that HSCs are the predominant cell type through which 5-HT$_{2B}$ negatively influences hepatocyte proliferation. However, as there are currently no proven genetic targeting systems to achieve HSC-specific deletion of the gene encoding 5-HT$_{2B}$, we cannot unequivocally rule out minor contributions from other cell types expressing 5-HT$_{2B}$.

We next investigated the intracellular signaling pathways through which serotonin and 5-HT$_{2B}$ mediate their antiregenerative effects. Transcription of *TGFB1* is under the control of the AP-1 transcription factor, a heterodimer of Jun and Fos family proteins. In activated HSCs, the predominant Jun isoform is JunD, whose activity in this cell type is controlled by ERK-mediated phosphorylation[22-24]. Using chromatin immunoprecipitation (ChIP) assays, we found that serotonin stimulates recruitment of JunD to AP-1 binding sites in the distal and proximal promoter regions of *Tgfb1* in rat and mouse HSCs (Fig. 3g and Supplementary Fig. 5a,b). Antagonism of 5-HT$_{2B}$ suppressed serotonin-induced recruitment of JunD, as did treatment of HSCs with the ERK inhibitor PD98059. Treatment with serotonin stimulated phosphorylation of ERK1 and ERK2 in rat (Fig. 3h), mouse and human HSCs (Supplementary Fig. 5c,d), and this response was inhibited by treatment with either PD98059 or SB-204741. Serotonin also induced phosphorylation of JunD, which was suppressed by treatment with PD98059 or SB-204741 (Fig. 3h). On the basis of these data, we propose that phosphorylation and activation of JunD by ERK mediates the stimulation of TGF-β1 transcription by serotonin and 5-HT$_{2B}$ in HSCs (Fig. 3i). If this pathway operates in the context of the injured liver, then JunD would be predicted to function as a transcriptional repressor of hepatocyte proliferation. Analysis of PCNA staining of liver sections from *Jund*$^{-/-}$ mice recovering from CCl_4 injury showed a higher number of mitotic hepatocytes compared to wild-type mice (Fig. 3j) associated with reduced TGF-β1 expression (Supplementary Fig. 5e). A similar suppressive role of JunD in epithelial cell proliferation has previously been reported in a model of partial nephrectomy, which was attributed to the suppression of TGF-α and epidermal growth factor receptor (EGFR) signaling in tubular epithelial cells[25].

Recent studies in the kidney have suggested that growth-arrested epithelial cells stimulate fibrogenesis by secreting TGF-β1, which, in this context, stimulates the fibrogenic activities of myofibroblasts[26]. Therefore, we determined whether antagonism of 5-HT$_{2B}$ exerts an antifibrogenic effect in a model of progressive liver disease in which both fibrogenesis and regeneration actively remodel the hepatic architecture. We gave mice CCl_4 injections twice weekly for 3 weeks to establish fibrotic disease prior to continuing with CCl_4 injury for a further 5 weeks with or without SB-204741 (Fig. 4a). Treatment with SB-204741 significantly reduced the number of hepatic α-SMA$^+$ fibrogenic cells (Fig. 4b), fibrotic matrix (Fig. 4c), hepatic expression of TGF-β1 (Fig. 4d) and expression of the fibrogenic genes encoding TIMP-1 and pro-collagen I, confirming an antifibrogenic effect at the molecular level (Fig. 4e,f). To corroborate these findings, we also determined the effects of treatment with SB-204741 in the model of progressive BDL-induced liver disease and observed a protective antifibrotic influence (Fig. 4g), as well as an improvement in liver function, as assessed by reduced concentrations of the serum transaminases ALT and AST (Fig. 4h). Furthermore, immunohistochemical analysis of caspase 3 activity in the CCl_4 model indicated that treatment with SB-204741 was associated with a higher rate of cellular apoptosis in the fibrotic matrix, which is indicative of enhanced tissue remodeling (Supplementary Fig. 5f). Activated human HSCs express 5-HT$_{2B}$, whereas human

hepatocytes do not (Supplementary Fig. 5g); hence, the mechanisms we describe have potential to operate in the diseased human liver.

Our understanding of the molecular regulation of liver regeneration is primarily derived from studies of healthy liver. Here we have addressed the additional regulatory complexity that could be relevant for regeneration in the context of the diseased liver and, specifically, a signaling network established by 5-HT_{2B}-expressing activated HSCs, which are abundant in chronic liver disease. It was originally reported that in healthy liver, platelet-derived serotonin promotes liver regeneration and that this function requires the activity of the 5-HT_2 subclass of receptors and, specifically, 5-HT_{2A}, which is expressed in hepatocytes[16]. However, expression of 5-HT_{2B} is relatively low in healthy liver as compared to diseased liver, in which this receptor is highly expressed in activated HSCs in association with fibrotic tissue[18]. We found that HSCs are key suppressors of hepatocyte proliferation and that this function is provided by serotonin-induced expression of TGF-β1, dependent on the 5-HT_{2B} receptor (Supplementary Fig. 6). Consequently, in the pathophysiological setting of ongoing fibrogenesis, the regenerative influence of serotonin acting through 5-HT_{2A} receptors on hepatocytes is subject to opposing antiregenerative effects arising from serotonin acting through 5-HT_{2B} receptors on HSCs. Additionally, we suggest that this paracrine signaling pathway can provide feedback to HSCs to further provoke their fibrogenic activities. In the context of normal hepatic wound repair, 5-HT_{2B}-mediated expression of TGF-β by activated HSCs presumably contributes to termination of parenchymal cell proliferation, which is involved in limiting the regenerative response to prevent overgrowth. With prolonged liver injury, apoptotic clearance of activated HSCs occurring during the resolving phase of wound repair would favor regenerative serotonin signaling via 5-HT_{2A} receptors on hepatocytes. Only when activated HSCs persist and become proliferative in progressive fibrogenesis would antiregenerative serotonin signaling via 5-HT_{2B} exert a pathological influence.

5-HT_{2B} is selectively expressed by activated human HSCs and the signaling pathway we describe here is conserved in human HSCs. Potent and selective antagonists of 5-HT_{2B} are already available and have been reported as being safe for clinical use in humans[27]. This class of drug may therefore have therapeutic potential in liver disease, both as stimulants of hepatocyte regeneration and as anti-fibrotic agents.

METHODS

Methods and any associated references are available in the online version of the paper at http://www.nature.com/naturemedicine/.

ONLINE METHODS

Mouse and liver injury and regeneration models

Mouse experiments were approved by the Newcastle Ethical Review Committee and performed under a UK Home Office license. Experiments using *Htr2b*$^{-/-}$ mice were conducted within institutional guidelines and European regulations. *Htr2b*$^{-/-}$ mice were on a 129/PAS background, and *Jund*$^{-/-}$ mice were on a mixed C57Bl6/129Sv background[24,28]. We administered either SB-204741 or ketanserin (3 mg per kg of body weight: Tocris Biochemicals) or vehicle (saline with 0.01% DMSO) i.p. to age-matched C57BL/6 mice for the 5-HT_2 antagonist studies. We performed PHX according to the method of Higgins and Anderson[29] and gave drugs daily in this model, with BrdU (150 mg per kg of body weight) given by i.p. injection 2 h before culling. For the models of PHX either with or without C1-3 or C1-3-gliotoxin, we gave antibodies at 2 mg per kg of body weight at 24 h and 48 h after surgery. We performed BDL as previously described[30] and administered SB-204741 daily

from day 7 until day 14 after surgery. We depleted HSCs during BDL using the single-chain antibody C1-3 conjugated to gliotoxin, as previously reported[13]. For treatment with acute CCl_4, we gave mice SB-204741, ketanserin or vehicle by i.p. injection 2 h before i.p. administration of a high-dose of CCl_4 (2 μl of CCl_4: olive oil (1:1 (v/v)) per g of body weight). We gave a second dose of 5-HT_2 antagonists or vehicle at 22 h and culled mice at 24 h after injury. For treatment with acute high doses of CCl_4 with or without C1-3 or C1-3-gliotoxin, with or without SB-204741, we administered the therapeutic agents 24 h and 40 h after injury. For treatment with chronic CCl_4, we injected mice, i.p. biweekly, with CCl_4 (2 μl of CCl_4: olive oil (1:3 (v/v)) per g of body weight) for 8 weeks to induce fibrosis. Three weeks after the initial CCl_4 injection we gave triweekly i.p. injections of SB-204741 or vehicle.

Primary liver cell isolation and culture

We isolated and cultured HSCs from male Sprague-Dawley rats and C57BL/6 mice as previously reported[24,29,31]. Ethical approval was granted by the Newcastle Ethical Review Committee, and experiments were performed under a UK Home Office license. We isolated human HSCs and hepatocytes from the normal margins of livers resected for removal of metastatic colorectal tumors with the full ethical consent of the subjects[12]. Unless otherwise stated, we treated the HSCs with 5 μM serotonin with or without 100 μM SB-204741 or 25 μM PD98059. Protocols for the isolation of mouse hepatocytes, HSCs, Kupffer cells and cholangiocytes are described in the Supplementary Methods.

Sirius red staining and immunohistochemistry

Staining was performed on formalin-fixed liver sections. We performed Sirius red, PCNA, BrdU and α-SMA staining as previously described[30]. We blocked endogenous peroxidase activity and achieved antigen retrieval using citric saline for immunohistochemical detection of Ki67, AFP, Gli2, CK19 and active caspase-3. For detection of 5-HT_{2B}, we combined citric saline and trypsin antigen retrieval and permeabilized the tissue with 0.5% Triton. For detection of F4/80, we used proteinase K antigen retrieval. We blocked tissue using an Avidin/Biotin Blocking Kit (Vector Laboratories) followed by addition of 20% swine serum in PBS. We incubated sections with primary antibodies to Ki67 (Novacastra; rabbit, 1:1,000), AFP (Dako; rabbit, 1:75), Gli2 (GenWay Biotech; rabbit, 1:500), CK19 (Abcam; rabbit, 1:250), 5-HT_{2B} (BD Pharminogen; mouse, 1:200), F4/80 (Abcam; rat, 1:100) and active caspase 3 (Cell Signaling Technology; rabbit, 1:200) overnight at 4 °C. We incubated sections with biotin-conjugated secondary antibody (Dako; 1:1,000) for 2 h, washed and incubated them with streptavidin biotin-peroxidase complex (Vector Laboratories) and visualized cells positive for the antibody using 3,3′-diaminobenzidine tetrahydrochloride staining. We manually counted the immunostained cells and calculated the mean number of positive cells per field in 15-20 high power (×20) fields. Data are means ± s.e.m. We used Leica QWin for morphometric analyses of the images.

Immunocytochemistry

We isolated HSCs from C57BL/6 mice 72 h after PHX and cultured them for 2 h on coverslips. We formalin fixed the cells, blocked them, and incubated them with antibodies to 5-HT_{2B} (Acris; rabbit, 1:100) overnight at 4 °C. We probed cells with an Alexa Fluor-594–conjugated mouse rabbit secondary antibody for 2 h and counterstained them with DAPI.

qRT-PCR

We isolated total RNA from ~200 μg of mouse liver or cultured cells using the Total RNA Purification Kit (QIAGEN). We treated the total RNA with DNAse and used it as a template in first strand complementary DNA synthesis using random primers (Promega). We

performed SYBR Green qRT-PCR as previously reported[30]. The primers used are listed in Supplementary Table 1.

SDS-PAGE and immunoblotting

We fractionated total protein by 9% SDS-PAGE and then transferred it onto nitrocellulose. We blocked blots with Tris-buffered saline and Tween 20 (0.1%) containing 5% BSA before incubation overnight with primary antibodies to ERK1, ERK2, phospho-ERK1 and phospho-ERK2 (Cell Signaling Technology; rabbit, 1:1,000), JunD (Santa Cruz; rabbit, 1:500), phospho-JunD (Upstate; rabbit, 1:500) and $5HT_{2B}$ (BD; mouse, 1:500). We washed membranes in T-TBS and incubated them with mouse antibody to rabbit IgG conjugated to horseradish peroxidase (Santa Cruz, 1:2,000) or mouse Trueblot (1:5,000) for 2 h. We washed the blots and detected the antigen by enhanced chemiluminescence (Amersham Biosciences).

ChIP assay

We treated activated rat or mouse HSCs for 30 min with SB-204741 or PD98059 and then stimulated them with 5-HT for 4 h. We prepared crosslinked chromatin using the protocol outlined in the Upstate Biotechnology Immunoprecipitation ChIP assay kit. We performed ChIP on 100 μg of crosslinked chromatin per reaction. We used 10 μg of antibody to JunD or non-specific IgG control (Abcam) for immunoprecipitation. We amplified the rat and mouse TGF-β1 promoters by qRT-PCR using specific primers (Supplementary Table 1).

Statistical analyses

We used GraphPad InStat to perform ANOVA and $P < 0.05$ was indicative of significance.

Additional methods

Detailed methodology is described in the Supplementary Methods.

Supplementary Material

Refer to Web version on PubMed Central for supplementary material.

Acknowledgments

This work was funded by grants from the UK Medical Research Council (grant G0700890 to D.A.M., M.C.W. and F.O. and G0900535 to F.O.), the Wellcome Trust (grant WT084961MA to F.O., D.A.M. and M.C.W. and WT086755MA to M.C.W., A.D.B. and D.A.M.). Work in D.A.M.'s lab is also funded by a European Commission FP7 program grant 'INFLA-CARE' (EC Contract No. 223151; http://inflacare.imbb.forth.gr/). M.R.E. was supported by a European Association for Study of the Liver (EASL) Sheila Sherlock fellowship. L.M.'s work was supported by the Centre National de la Recherche Scientifique, the Institut National de la Santé et de la Recherche Médicale, the Université Pierre et Marie Curie and by grants from the Fondation de France, the Fondation pour la Recherche Médicale, the French ministry of research (Agence Nationale pour la Recherche) and the European Commission (DEVANX).

References

1. Gurtner GC, Werner S, Barrandon Y, Longaker MT. Wound repair and regeneration. Nature. 2008; 453:314–321. [PubMed: 18480812]
2. Wallace K, Burt AD, Wright MC. Liver fibrosis. Biochem. J. 2008; 411:1–18. [PubMed: 18333835]
3. Marshall A, et al. Relation between hepatocyte G1 arrest, impaired hepatic regeneration, and fibrosis in chronic hepatitis C virus infection. Gastroenterology. 2005; 128:33–42. [PubMed: 15633121]
4. Roskams T. Liver stem cells and their implication in hepatocellular and cholangiocarcinoma. Oncogene. 2006; 25:3818–3822. [PubMed: 16799623]

5. Malik R, Selden C, Hodgson H. The role of non-parenchymal cells in liver growth. Semin. Cell Dev. Biol. 2002; 13:425–431. [PubMed: 12468243]
6. Friedman SL. Hepatic stellate cells: protean, multifunctional, and enigmatic cells of the liver. Physiol. Rev. 2008; 88:125–172. [PubMed: 18195085]
7. Passino MA, Adams RA, Sikorski SL, Akassoglou K. Regulation of hepatic stellate cell differentiation by the neurotrophin receptor p75NTR. Science. 2007; 315:1853–1856. [PubMed: 17395831]
8. Kalinichenko VV, et al. Foxf1$^{+/-}$ mice exhibit defective stellate cell activation and abnormal liver regeneration following CCl4 injury. Hepatology. 2003; 37:107–117. [PubMed: 12500195]
9. Scobie BA, Summerskill WH. Hepatic cirrhosis secondary to obstruction of the biliary system. Am. J. Dig. Dis. 1965; 10:135–146. [PubMed: 14258249]
10. Polimeno L, et al. Cell proliferation and oncogene expression after bile duct ligation in the rat: evidence of a specific growth effect on bile duct cells. Hepatology. 1995; 21:1070–1078. [PubMed: 7705781]
11. Wright MC, et al. Gliotoxin stimulates the apoptosis of human and rat hepatic stellate cells and enhances the resolution of liver fibrosis in rats. Gastroenterology. 2001; 121:685–698. [PubMed: 11522753]
12. Elrick LJ, et al. Generation of a monoclonal human single chain antibody fragment to hepatic stellate cells—a potential mechanism for targeting liver anti-fibrotic therapeutics. J. Hepatol. 2005; 42:888–896. [PubMed: 15885360]
13. Douglass A, et al. Antibody-targeted myofibroblast apoptosis reduces fibrosis during sustained liver injury. J. Hepatol. 2008; 49:88–98. [PubMed: 18394744]
14. Cassiman D, Libbrecht L, Desmet V, Denef C, Roskams T. Hepatic stellate cell/myofibroblast subpopulations in fibrotic human and rat livers. J. Hepatol. 2002; 36:200–209. [PubMed: 11830331]
15. Omenetti A, et al. Hedgehog-mediated mesenchymal-epithelial interactions modulate hepatic response to bile duct ligation. Lab. Invest. 2007; 87:499–514. [PubMed: 17334411]
16. Lesurtel M, et al. Platelet-derived serotonin mediates liver regeneration. Science. 2006; 312:104–107. [PubMed: 16601191]
17. Omenetti A, et al. Paracrine modulation of cholangiocyte serotonin synthesis orchestrates biliary remodeling in adults. Am. J. Gastrointest. Liver Physiol. 2011; 300:G303–G315.
18. Ruddell RG, et al. A role for serotonin (5-HT) in hepatic stellate cell function and liver fibrosis. Am. J. Pathol. 2006; 169:861–876. [PubMed: 16936262]
19. Forbes IT, Jones GE, Murphy OE, Holland V, Baxter GS. N-(1-methyl-5-indolyl)-N′-(3-methyl-5-isothiazolyl)urea: a novel, high-affinity 5-HT2B receptor antagonist. J. Med. Chem. 1995; 38:855–857. [PubMed: 7699699]
20. Varty GB, Higgins GA. Reversal of dizocilpine-induced disruption of prepulse inhibition of an acoustic startle response by the 5-HT2 receptor antagonist ketanserin. Eur. J. Pharmacol. 1995; 287:201–205. [PubMed: 8749037]
21. Fausto N. Protooncogenes and growth factors associated with normal and abnormal liver growth. Dig. Dis. Sci. 1991; 36:653–658. [PubMed: 2022167]
22. Kim SJ, et al. Autoinduction of transforming growth factor β 1 is mediated by the AP-1 complex. Mol. Cell. Biol. 1990; 10:1492–1497. [PubMed: 2108318]
23. Smart DE, et al. JunD regulates transcription of the tissue inhibitor of metalloproteinases-1 and interleukin-6 genes in activated hepatic stellate cells. J. Biol. Chem. 2001; 276:24414–24421. [PubMed: 11337499]
24. Smart DE, et al. JunD is a profibrogenic transcription factor regulated by Jun N-terminal kinase-independent phosphorylation. Hepatology. 2006; 44:1432–1440. [PubMed: 17133482]
25. Pillebout E, et al. JunD protects against chronic kidney disease by regulating paracrine mitogens. J. Clin. Invest. 2003; 112:843–852. [PubMed: 12975469]
26. Yang L, Besschetnova TY, Brooks CR, Shah JV, Bonventre JV. Epithelial cell cycle arrest in G2/M mediates kidney fibrosis after injury. Nat. Med. 2010; 16:535–543. [PubMed: 20436483]

27. Palmer MJ. Leads for the treatment of pulmonary hypertension. Expert Opin. Ther. Pat. 2009; 19:575–592. [PubMed: 19441935]
28. Nebigil CG, et al. Serotonin 2B receptor is required for heart development. Proc. Natl. Acad. Sci. USA. 2000; 97:9508–9513. [PubMed: 10944220]
29. Higgins GM, Anderson RM. Experimental pathology of the liver I. Restoration of the liver of white rat following partial surgical removal. Arch. Pathol. 1931; 12:186–202.
30. Gieling RG, et al. The c-Rel subunit of nuclear factor-κB regulates murine liver inflammation, wound-healing, and hepatocyte proliferation. Hepatology. 2010; 51:922–931. [PubMed: 20058312]
31. Arthur MJ, Friedman SL, Roll FJ, Bissell DM. Lipocytes from normal rat liver release a neutral metalloproteinase that degrades basement membrane (type IV) collagen. J. Clin. Invest. 1989; 84:1076–1085. [PubMed: 2551922]

Europe PMC Funders Author Manuscripts

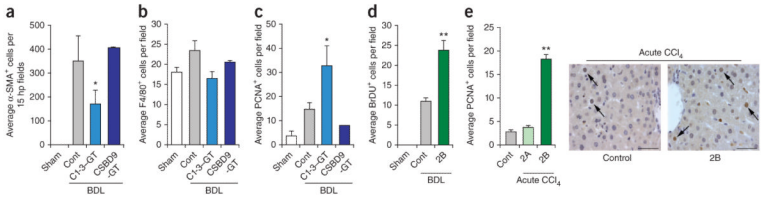

Figure 1.

Selective depletion of hepatic stellate cells or antagonism of 5-HT_{2B} stimulates liver growth. (**a–c**) The average number of α-SMA^+ myofibroblasts (**a**), $F4/80^+$ Kupffer cells (**b**) and $PCNA^+$ hepatocytes (**c**) per field, or set of fields, in liver tissue samples from mice that underwent BDL followed by intraperitoneal (i.p.) injections of C1-3–gliotoxin (C1-3–GT), control antibody conjugated to gliotoxin (CSBD9-GT) or saline vehicle (Cont) or from mice that underwent a sham operation without further treatment. (**d**) Average BrdU-stained hepatocytes per field in liver tissue samples from mice that underwent BDL followed by i.p. injections of the 5-HT_{2B} antagonist SB-204741 (2B) or vehicle (Cont) versus sham operation with no further treatment. (**e**) Left, the average number of $PCNA^+$ hepatocytes per field in liver tissue samples from mice i.p. injected with CCl_4 followed by i.p. administration of vehicle (Cont), 5-HT_{2A} antagonist ketanserin (2A) or the 5-HT_{2B} antagonist SB-204741 (2B). Right, representative images of PCNA-stained liver; arrows denote $PCNA^+$ hepatocytes. Error bars are means ± s.e.m. Data are representative of four or five mice per group. $*P < 0.05$, $**P < 0.01$ compared to control, calculated using analysis of variance (ANOVA). Scale bars, 50 μm. Hp, high power.

Europe PMC Funders Author Manuscripts

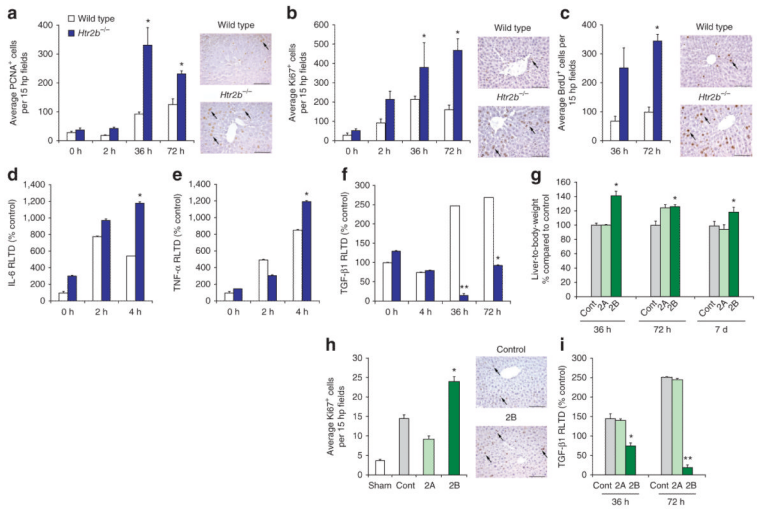

Figure 2.

Gene deletion or blockade of 5-HT_{2B} enhances liver regeneration after PHX. (**a–c**) Average number of $PCNA^+$ (**a**), $Ki67^+$ (**b**) and $BrdU^+$ (**c**) hepatocytes, per 15 hp fields, in liver sections from wild-type (WT) or *Htr2b* (5-HT_{2B} receptor)-knockout mice that underwent PHX or a sham operation. Representative images of PCNA, Ki67 and BrDU immunostaining; arrows denote positively stained hepatocytes. (**d–f**) Whole-liver IL-6 (**d**), TNF-α (**e**) and TGF-β1 (**f**) mRNA levels expressed as relative level of transcription difference (RLTD) at the indicated time points after PHX in WT and knockout mice. (**g**) Liver-to-body-weight ratio in mice that underwent PHX followed by i.p. injections of vehicle (Cont), ketanserin (2A) or SB-204741 (2B). (**h,i**) The average number of $Ki67^+$ hepatocytes per 15 hp fields (**h**) and whole-liver TGF-β1 mRNA levels (**i**) in mice that underwent PHX followed by i.p. administration of vehicle (Cont), ketanserin (2A), SB-204741(2B) or sham operation. Representative images of Ki67-stained liver; arrows denote $Ki67^+$ hepatocytes. All images are at ×200 magnification; scale bars, 100 μm. Data are means ± s.e.m. and representative of at least four mice per group. Statistical significance was determined by ANOVA, $*P < 0.05$, $**P < 0.01$ compared to control, 0 h or 36 h.

Europe PMC Funders Author Manuscripts

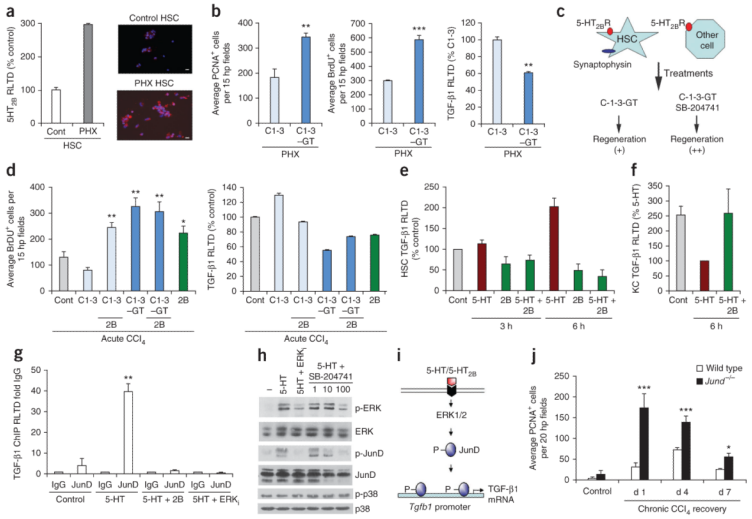

Figure 3.

5-HT_{2B} blockade enhances liver regeneration by inhibiting induction of TGF-β1 expression by HSC that is dependent on 5-HT, ERK and JunD. (**a**) Expression of 5-HT_{2B} determined by immunocytochemistry and qRT-PCR (RLTD) in HSCs isolated from the liver of control mice or 36 h PHX mice; $n = 3$ cell preparations. Scale bars, 10 μm. (**b**) Average number of $PCNA^+$ and $BrDU^+$ hepatocytes per 15 hp fields and TGF-β1 mRNA levels in mice treated with C1-3 or C1-3–gliotoxin 72 h after PHX. (**c**) Experiment to determine whether HSCs mediate the regenerative effects of 5-HT_{2B} antagonism. If other cells expressing 5-HT_{2B} are involved, then the combination of C1-3-GT–induced HSC apoptosis and treatment with SB-204741 should generate additive (++) effects compared with C1-3-GT treatment alone (+). (**d**) Average number of $BrdU^+$ hepatocytes per 15 hp fields and TGF-β1 mRNA levels in livers from mice i.p. injected with CCl_4 followed by i.p. administration of either C1-3 or C1-3–gliotoxin ± SB-204741 or vehicle. (**e,f**) TGF-β1 mRNA levels in mouse HSCs (**e**) or Kupffer cells (KC) (**f**) stimulated with 5-HT ± SB-204741. (**g**) ChIP analysis of JunD recruitment to the TGF-β1 promoter in rat HSCs stimulated with 5-HT for 4 h ± SB-204741 (2B) or ERK inhibitor PD98059 (ERK_i). (**h**) Western blot detection of ERK, phospho-ERK (p-ERK), JunD, phospho-JunD (p-JunD) and p38 or phospho-p38 (p-p38) in rat HSCs that had been pretreated for 30 min with PD98059 or 1–100 μM SB-204741 prior to stimulation with 5-HT. (**i**) Schematic representation of ERK-dependent recruitment of JunD to the TGF-β1 promoter in HSCs upon 5-HT binding to the 5-HT_{2B} receptor. (**j**) Average number of $PCNA^+$ hepatocytes in liver sections from WT and JunD-knockout mice at peak injury and recovery (days 1–7 after the final injection) after 8 weeks of CCl_4 injury. Data are means ± s.e.m. of at least four mice per group. $^*P < 0.05$, $^{**}P < 0.01$, $^{***}P < 0.001$ compared to control calculated by ANOVA.

Europe PMC Funders Author Manuscripts

Europe PMC Funders Author Manuscripts

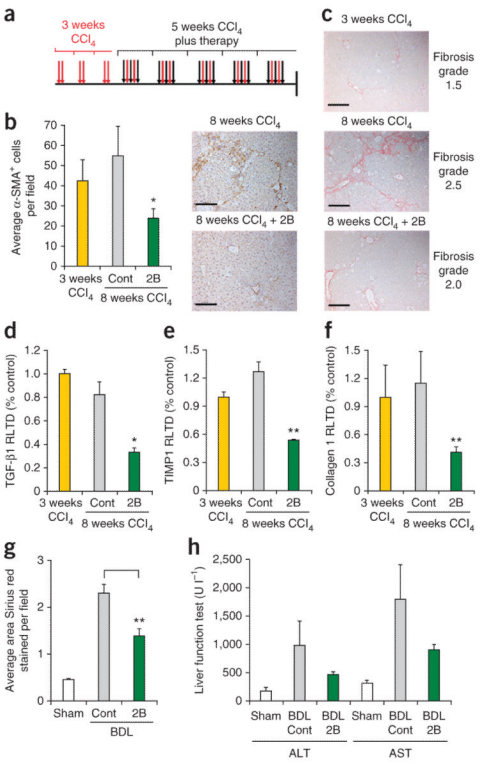

Figure 4.

Blockade of 5-HT_{2B} receptors attenuates liver fibrosis. (**a**) Diagram showing the dosing regime in the therapy model; mice were given CCl_4 injections i.p. biweekly for 3 weeks, followed by i.p. injections of SB-204741 (2B) or vehicle (Cont) triweekly in addition to biweekly CCl_4 for a further 5 weeks. (**b**) Average number of α-SMA^+ cells per hp field and representative images of α-SMA–immunostained liver sections in this model. (**c**) Fibrosis pathology scoring using the adapted Metavir scale and representative images of livers stained with Sirius red (collagen deposition) in this model. (**d–f**) Whole-liver TGF-β1, tissue inhibitor of metalloproteinase 1 (TIMP1) and collagen I mRNA levels (RLTD) in this model. (**g**) Mice underwent BDL, followed by i.p. injections of SB-204741 or vehicle (Cont) daily for 7 d starting at day 7 after BDL. The average Sirius red-positive area per field was calculated using morphometric analysis. (**h**) Serum transaminases, alanine transaminase (ALT) and aspartate transaminase (AST), markers of liver function, were assessed at 14 d after BDL ± SB-204741 or after sham operation. Photomicrographs are at ×100 magnification. Scale bars, 100 μm. Data are means ± s.e.m. $n = 5$ mice per group. $^*P < 0.05$, $^{**}P < 0.01$ compared to control calculated by ANOVA.